Pilot-Based TI-ADC Mismatch Error Calibration for IR-UWB Receivers

Christian A. Schmidt, Jose L. Figueroa, Juan E. Cousseau, Andrea M. Tonello

Date of publication xxxx 00, 0000, date of current version xxxx 00, 0000.

Digital Object Identifier 10.1109/ACCESS.2017.DOI

Pilot-based TI-ADC Mismatch Error Calibration for IR-UWB Receivers

CHRISTIAN A. SCHMIDT[12], JOSÉ L. FIGUEROA[1], JUAN E. COUSSEAU[1], and ANDREA M. TONELLO.[3]

[1]Instituto de Investigaciones en Ingeniería Eléctrica - CONICET - Universidad Nacional del Sur, Bahía Blanca, Argentina (e-mails: [cschmidt,figueroa,jcousseau]@uns.edu.ar)

[2]Univ. Rennes, INSA Rennes, IETR, UMR-CNRS 6164, 35000 Rennes, France.

[3]Institute of Networked and Embedded Systems - Alpen-Adria-Universität Klagenfurt, Austria (e-mail: andrea.tonello@aau.at)

Corresponding author: C. A. Schmidt (e-mail: cschmidt@uns.edu.ar).

ABSTRACT In this work, we first provide an overview of the state of the art in mismatch error estimation and correction for time-interleaved analog to digital converters (TI-ADCs). Then, we present a novel pilot-based on-line adaptive timing mismatch error estimation approach for TI-ADCs in the context of an impulse radio ultra wideband (IR-UWB) receiver with correlation-based detection. We introduce the developed method and derive the expressions for both additive white Gaussian noise (AWGN) and Rayleigh multipath fading (RMPF) channels. We also derive a lower bound on the required ADC resolution to attain a certain estimation precision. Simulations show the effectiveness of the technique when combined with an adequate compensator. We analyze the estimation error behavior as a function of signal to noise ratio (SNR) and investigate the ADC performance before and after compensation. While all mismatches combined cause the effective number of bits (ENOB) to drop to 3 bits and to 6 bits when considering only timing mismatch, estimation and correction of these errors with the proposed technique can restore a close to ideal behavior. We also show the performance loss at the receiver in terms of bit error rate (BER) and how compensation is able to significantly improve performance.

INDEX TERMS Analog-digital conversion, Error correction, Receivers, Ultra wideband technology.

I. INTRODUCTION

IMPULSE radio ultra wideband technologies have become an interesting solution for many applications such as localization, power line communications (PLC), high data-rate and low-range communications, sensor networks, among others [1], [2], [3].

As a consequence of its wide spectrum, UWB communication systems can have bandwidths of up to several GHz. There exists therefore an ever increasing demand for high performance, high-speed analog-to-digital converters (ADCs) in order to comply with the sampling requirements of IR-UWB (and other modern wideband communications systems and standards like LTE, 5G, optic transceivers, and cognitive radio) [4], [5], [6], [7]. However, there is also traditionally a trade-off between the achievable resolution and sampling speed [4], [8]. Among the alternatives, TI-ADCs are a promising solution that has become a trend and an active research topic, as they are key to sample the signals at the required rates.

A TI-ADC is an array composed of several (say M) ADCs working in parallel with time-shifted sampling clocks such that the overall effective sampling rate is proportionally increased. However, due to inaccuracies inherent to the manufacturing process that prevent the component ADCs from being exactly equal to each other, there are specific mismatches that can severely deteriorate the performance of the whole system. Thus, addressing three typical mismatches: gain, offset and timing skew, estimation and correction is required [4], [8], [9], [10]. Gain mismatch errors occur when the amplitude ratio between analog input and digital output differs for each ADC, whereas offset mismatch is due to different DC values at their output (even when the input is set to zero). Finally, timing mismatch errors cause the output signal to be periodically but non-uniformly sampled [11], [12]. Unlike offset and gain mismatches, which are static, distortion due to timing mismatch is dynamic (i.e. signal dependent) and requires additional signal processing with higher computational complexity. While offset and gain mismatches are quite straightforward to estimate and cancel [13], [11], background on-line timing mismatch estimation remains a challenge and motivates active research [6], [14]–

[19].

A. STATE-OF-THE ART ON MISMATCH COMPENSATION

In order to reduce the mismatch errors distortion effects, two tasks must be performed. First, an accurate estimation of the mismatch errors must be obtained. Then, this information can be used to apply an adequate compensation technique. The mismatch error estimation phase is the most critical part, i.e. the estimation error must be as low as possible. Several alternatives have been recently proposed to tackle the problem [14], [15]. For instance, signal processing can be performed in the digital domain, or in both analog and digital domains (mixed mode solutions) [6], [16]. In [6], the mean squared error (MSE) of detection is measured in the digital domain, while delays on the clock paths to each ADC are adjusted in the analog domain through adjustable delay paths until the MSE is minimized. The main drawback of solutions involving analog processing is that they require additional hardware, whose precision set a bound to their estimation and correction capabilities. On the other hand, fully digital techniques only require additional digital processing and can thus be adapted to any ADC [16].

Another important distinction can be made based on weather the ADC operation must be interrupted or not during the parameter estimation process. Foreground (off-line) calibration relies on an additional training signal known a priori that is used to estimate the compensator parameters [16], [11]. This strategy results in more accurate estimates of the parameters involved, but operation must be (periodically) stopped. On the contrary, background (on-line) calibration techniques are capable of directly using the input signal during normal operation of the ADC for estimation and correction of distortion [17]. They can also be divided in blind or pilot-based methods. Blind methods do not require any information on the input signal. Instead, they use either an additional reference ADC or elaborated algorithms exploiting some system knowledge to design suitable cost functions and minimize them adaptively (normally using gradient-based methods) [17], [18]. While the advantage is the resulting great flexibility that can be achieved, their computational complexity can be very high, and they result in lower accuracy. For instance, in [18], the distortion part of the ADC output signal is estimated by doing several Hilbert transforms, frequency shifting and folding operations and an LMS algorithm for each channel ADC to minimize a cost function. In [19], estimation of timing mismatch is obtained through derivative filters, where an LMS algorithm using Taylor approximations is used for the cost function. In this case, the method is tested with a sampling frequency of 3.6 GHz and timing mismatch in the order of a few picoseconds, which implies that the method is accurate when the timing mismatch is low, in accordance with the results in [11], where it is shown that linear interpolation and spline interpolation are sufficient in this case. However, for larger timing mismatch, higher order interpolation techniques are needed. Finally, background on-line (adaptive or not) estimation and correction could also be obtained by means of pilot-based methods.

A pilot-based on-line calibration method could gather the advantages of both blind and foreground techniques. Pilot signals are transmitted signals known at the receiver that are used in systems and standards such as OFDM, IR-UWB, etc., for different tasks such as channel estimation, synchronization or carrier frequency offset estimation [20], [21], [22]. The idea behind this approach is to use these pilot tones or symbols along with any particular knowledge on the system itself to get on-line accurate estimates of the model parameters. While pilot-based estimation and its characteristics have been widely studied in certain applications, and particularly in the context of channel estimation and synchronization [20], [21], [22], to the best of our knowledge this approach has not yet been implemented for estimation and correction of mismatch errors in TI-ADCs. In this work, we propose a pilot-based estimation technique for TI-ADC mismatch error calibration, and analyze its performance. We show that it enables lower computational complexity and higher accuracy when compared to blind methods, as well as tracking capabilities to changes in the parameters while maintaining normal operation of the sampling stage as opposed to foreground calibration.

B. PAPER CONTRIBUTION

In this paper, we propose a novel pilot-based on-line mismatch error estimation algorithm in TI-ADCs for an IR-UWB receiver with reduced complexity. In particular, we propose to use an average of the received pulses to estimate the TI-ADC mismatch parameters. Then, we use the mismatch estimates to implement the compensation method in [11], which has already been tested both by simulations and experimental verification. Finally, correlation based data detection is performed between the compensated signal and a clean template. We analyze the results in terms of system performance metrics, such as bit error rate (BER), as well as ADC performance metrics, as signal to noise and distortion ratio (SINAD), showing that after compensation a significant improvement can be obtained. We previously showed in [11] both by simulations and measurements that the correction method presents excellent results in compensation performance provided that estimation accuracy of the mismatch parameters is good enough. In this work, we show that high-quality estimates can also be obtained by the newly proposed method.

The manuscript provides the following contributions:

- We propose a novel low complexity on-line estimation method for mismatch errors in a time-interleaved ADC suitable for IR-UWB receivers. Unlike foreground off-line estimation methods with sine-wave training signals (and thus, computationally intensive sine-wave fitting algorithms), the novel estimation method is based on the received signal itself (avoiding the use of external calibration signals).

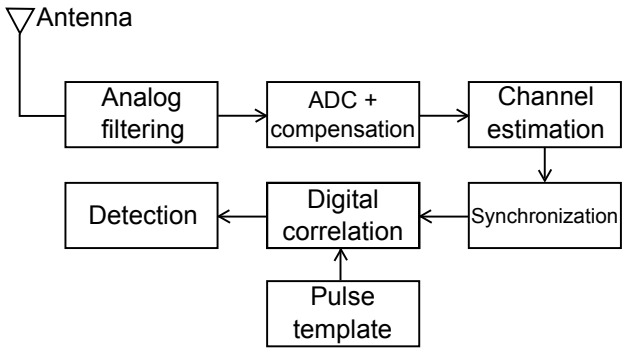

FIGURE 1. Block diagram of the receiver.

- The proposed method is able to cope with changes in the mismatch parameters through tracking. Hence, periodical estimation is not needed and the ADC operation is not interrupted. In addition, we derive the expression on the lower bound of the required ADC resolution in order to attain a certain estimation precision.
- We analyze different aspects of sampling for an IR-UWB receiver and their effect on detection performance, including ADC resolution, and ADC induced distortion considering typical wireless communication channels. We show that the proposed estimation method gives accurate results that are capable of restoring adequate performance when combined with an efficient compensation block.

This work is organized as follows. A brief model of the IR-UWB receiver is introduced in Section II, where the transmitted signal, the channel model, and pulse waveform used are described. In Section III, the TI-ADC structure is presented along with gain and offset mismatch estimation methods. A novel background timing mismatch error estimation technique is presented in Section IV, where the method is introduced and a lower bound on the required ADC resolution is also derived. Compensation using the obtained estimates is briefly described in Section V. Section VI provides a comparative analysis with current state of the art proposals. Simulation results of the ADC and receiver performance in terms of SINAD and BER are shown in Section VII, where the effect of ADC resolution and ADC induced distortion for the case of a TI-ADC are considered. A post-compensator for mismatch errors following the approach used in [11] is used to test the accuracy of the estimation technique. Finally, some conclusions are given in Section VIII.

II. IR-UWB RECEIVER MODEL

Fig. 1 shows the block diagram of an IR-UWB receiver and the processing chain. The signal is received at the antenna and filtered in the analog domain. Then, it is digitized by the ADC, which includes a compensation stage at its output to reduce distortion. After channel estimation and time synchronization, a digital correlation with the pulse template is performed for data detection.

IR-UWB transceivers transmit a train of ultra-short (and therefore ultra-wideband) pulses, which are then correlated with the pulse shape at the receiver side for detection. The transmitted signal is

$$x(t) = \sum_{k=0}^{N_F-1} b_k p(t - kT_r) \tag{1}$$

where $b_k \in \{-1, 1\}$ are the information bits, $p(t)$ is the transmission pulse, T_r is the pulse period (bit period), and N_F is the number of bits in the data frame. In this work, we use gaussian pulses as in [2],

$$p(t) = \frac{K_0}{\sqrt{2}T_0} e^{-\frac{\pi}{2}\left(\frac{t-t_0}{T_0}\right)^2} \tag{2}$$

where K_0 is proportional to the pulse energy and T_0 defines the bandwidth.

The performance study that we present involves two different channel models, an additive white gaussian noise (AWGN) channel, and a Rayleigh multipath fading (RMPF) channel. We consider these two channels to serve as best and worst case scenarios to get insight in the performance of the system. The receiver structure used for the case of an AWGN channel is a matched filter (MF). When transmitting over a RMPF channel, which is representative of many radio communication scenarios when reflections and scattering are present, we use a rake receiver with maximum ratio combining (MRC) [23], [24]. The received signal is

$$r(t) = x(t) * h(t) + \eta(t) \tag{3}$$

where $\eta(t)$ is AWGN and $h(t)$ is the impulse response of the channel. In the case of an AWGN channel, $h(t) = \delta(t)$. For a RMPF channel

$$h(t) = \sum_{l=0}^{L-1} c_l(t)\delta(\tau - l/W) \tag{4}$$

where $L = T_m W + 1$ is the number of taps of the tapped delay equivalent channel, W is the signal bandwidth, T_m is the channel multipath spread, and $c_l(t)$ are the baseband complex time varying channel coefficients with Raylegh distributed amplitude and uniform distributed phase. We assume a pulse repetition time $T_r > T_m$ in order to avoid inter-symbol interference (ISI), with a guard time $T_g = T_r - T_m$. Then, since we have a resolution of $1/W$ in the multipath delay profile, we have L resolvable paths. Hence, a MRC receiver should achieve the performance of an equivalent Lth order diversity communication system [24]. The received signal in a time window covering the transmission pulse repetition rate T_r, assuming synchronization, channel estimation, and considering the kth transmitted bit is

$$r_k(t) = b_k \sum_{l=0}^{L-1} c_l(t)p(t - l/W) + \eta_k(t) \tag{5}$$

Then, the decision variable using a rake receiver with MRC is

$$U(kT_r) = \Re\left[\int_0^{T_r} r_k(t)v^*(t)\right] \tag{6}$$

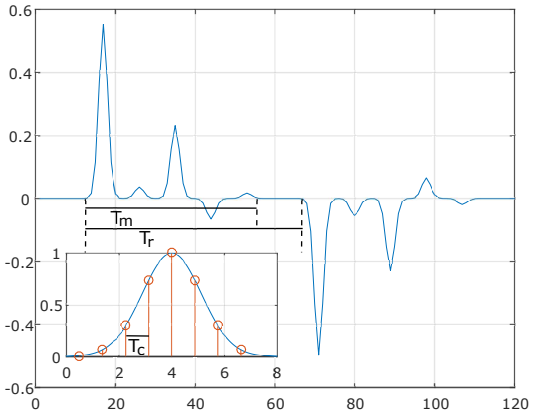

FIGURE 2. Received signal in a multipath channel for $L = 5$.

where $\Re[x]$ denotes the real part of x. Expanding $v^*(t) = \sum_{l=0}^{L-1} c_l^*(t)p^*(t - l/W)$ we get

$$U = \Re\left[\sum_{l=0}^{L-1}\int_0^{T_r} r_k(t)c_l^*(t)p^*(t - l/W)dt\right] \quad (7)$$

If we consider discrete-time processing [25], the received signal is sampled at the output of the RF front-end analog filter at sampling rate $T_c = T_r/N_S$, such that $N_S = ML$ samples are available to digitize the pulse and the received replicas, we get

$$r_k(nTc) = b_k\sum_{l=0}^{L-1} c_l(nT_c)p(nT_c - l/W) + \eta_k(nT_c) \quad (8)$$

with $n = 0, \cdots, N_S-1$. Then, the decision variable becomes

$$U = \Re\left[\sum_{l=0}^{L-1}\sum_{n=0}^{N_S-1} T_c r_k(nT_c)c_l^*(nT_c)p^*(nT_c - l/W)\right] \quad (9)$$

and the estimated bit is

$$\hat{b}_k = \text{sign}[U] \quad (10)$$

where the sign function is defined as

$$\text{sign}(x) = \begin{cases} -1, & x < 0 \\ 0, & x = 0 \\ 1, & x > 0 \end{cases} \quad (11)$$

If the sampling frequency is $f_c = 1/T_c = 2W$, it is the Nyquist samplig rate f_N. Otherwise, if $f_c > f_N$ there is oversampling, and more terms are added to the decision metric. As a consequence, the correlation with the pulse template $p(nT_c)$ is more robust and the equivalent quantization noise is reduced, leading to an improvement in BER performance. A similar analysis is possible for the AWGN channel replacing (4) by $h(t) = \delta(t)$. Figure 2 shows two received bits affected by a multipath channel, where T_r, T_m and T_c are depicted.

III. MISMATCH ERRORS IN A TI ADC

Unfortunately, due to fabrication process inaccuracies, any TI-ADC architecture presents gain, offset, and timing mismatch errors between the different ADC channels, which lead to a non ideal behavior [8]. Offset mismatch is caused by different DC levels at each ADC ouput, whereas gain mismatch results when the gain from the analog input to the digital output is different for each ADC in the interleaved array. Timing mismatch is due to a static phase shift Δt_m in the clock of ADC m, which results in deviation of the sampling instant (and hence an amplitude error in the sample taken). This error is more critical since it depends on the dynamics of the input signal, and its compensation requires some extra digital signal processing.

Let $r(t)$ be the received signal and T_c the overall high speed sampling period, $T = MT_c$ the sampling period at each channel ADC, and $\tau_m^I = mT_c$ the ideal sampling shift for the mth ADC. Then, the ideally sampled signal without mismatch errors is

$$r_m^I(kT) = r^I(mT_c + kMT_c) = r_m^I(kMT_c) = r^I(nT_c) \quad (12)$$

with $m = 0, 1, \cdots, M-1$ and $k, n \in Z$, where $r_m^I(kMT_c)$ is the polyphase decomposition of the signal [26], and $nT_c = mT_c + kT$. If we add the gain, offset and timing mismatch errors G_m, O_m and Δt_m, we get

$$r_m(kT) = G_m(kT)r(mT_c + kMT_c + \Delta t_m) + O_m(kT) \quad (13)$$

If we define

$$\begin{aligned} G_m(kT) &= G(mT_c + kT) = G(nT_c) \\ O_m(kT) &= O(mT_c + kT) = O(nT_c), \end{aligned} \quad (14)$$

then

$$r_m(kT) = G_m(kT)[r_m^I(kT) + \Delta r_m(kT)] + O_m(kT) \quad (15)$$

Considering that $nT_c = mT_c + kT$, we can write the output of the TI ADC as,

$$r(nT_c) = G(nT_c)[r^I(nT_c) + \Delta r(nT_c)] + O_m(nT_c) \quad (16)$$

From here on, we use the notation $r_m[k]$ for $r_m(kT)$ and $r[n]$ for $r(nT_c)$.

Estimation of mismatch errors is required as a first step in order to compensate them. In addition, the quality of the estimates should be as high as possible while keeping low complexity for the compensation to be effective and feasible. According to [13], offset and gain errors can be adaptively estimated on-line by taking the mean and variance of the individual ADC outputs, respectively.

Then, considering a balanced source of information (i.e., the amount of transmitted ones and zeros is roughly equal), the input signal to the ADC has zero mean and the *offset* mismatch can be calculated by directly averaging K samples at the output of each channel ADC,

$$\hat{O}_m = \frac{1}{K}\sum_{k=1}^{K} r_m[k] \quad (17)$$

As for the *gain* mismatch, it can be computed as the variance of each ADC output,

$$\hat{G}_m = \frac{1}{K}\sum_{k=1}^{K}(r_m[k]-\mu)^2 \tag{18}$$

where $\mu = 0$ if we consider the offset has been previously canceled. In that case, (18) reduces to

$$\hat{G}_m = \frac{1}{K}\sum_{k=1}^{K}(r_m[k])^2 \tag{19}$$

otherwise, μ in eq. (18) can be computed using eq. (17). Note that both (17) and (18) can be adaptively updated (on-line) by adding the next sample $r_m[k+1]$ to the calculations. This enables not only on-line background estimation but also tracking capabilities to changes in the parameters that could arise due to temperature variations, aging, etc.

IV. NOVEL ON-LINE TIMING MISMATCH ERROR ESTIMATION

In this section, we propose an on-line background estimation method for timing mismatch errors for the IR-UWB receiver under consideration.

A. PROBLEM STATEMENT AND FORMULATION FOR AWGN AND RMPF CHANNELS

Let us begin with the case of a general communications channel under the assumptions in Section II and with a certain impulse response $h(t)$. Then, according to (1) and (3), the kth received bit can be expressed as

$$r_k(t) = b_k p(t-kT_r) * h(t) + \eta_k(t) \tag{20}$$

If we sample (20) with an ideal TI-ADC and a sampling period T_c, we get

$$r_k(nT_c) = b_k p(nT_c - kT_r) * h(nT_c) + \eta_k(nT_c) \tag{21}$$

with $n = 0, \cdots, N_S - 1$. We assume $N_S = ML$ where L is the number of taps of the taped delay equivalent channel, such that M samples are taken from each pulse replica, i.e. L samples for each channel in the TI-ADC. If we assume that gain and offset mismatch have already been estimated and compensated for, we can express the sampled signal with timing mismatch as

$$r_k(nT_c) = b_k p(nT_c - kT_r + \Delta t_n) * h(nT_c) + \eta_k(nT_c) \tag{22}$$

We now consider the case where a pilot training signal composed of K_P bits is available, which may be the same used for channel estimation and time synchronization. Assuming L resolvable paths, the estimated channel coefficients are used to recover the phase and amplitude of each pulse replica such that $h(nT_c)$ can be replaced by an impulse train

$$\tilde{h}(nT_c) = \sum_{l=0}^{L-1}\delta(t - lT_m/(L-1)) = \sum_{l=0}^{L-1}\delta(t - l/W) \tag{23}$$

We can thus add averaging and a multiplication by the known b_ks such that

$$\hat{r}(nT_c) = \frac{1}{K_P}\sum_{k=1}^{K_P} b_k^2 p(nT_c - kT_r + \Delta t_n) * \tilde{h}(nT_c) + \eta_k(nT_c) \tag{24}$$

As $b_k^2 = 1$, and η_k is a white Gaussian noise processes (with zero mean), the averaged pulses can be approximated as

$$\hat{r}(nT_c) \cong p(nT_c + \Delta t_n) \tag{25}$$

For the case of an AWGN channel, replacing $h(t) = \delta(t)$ in (20), the kth received bit can be expressed as

$$r_k(t) = b_k p(t - kT_r) + \eta_k(t) \tag{26}$$

In this case, sampling (26) with an ideal TI-ADC, (21) becomes

$$r_k(nT_c) = b_k p(nT_c - kT_r) + \eta_k(nT_c) \tag{27}$$

with $n = 0, \cdots, N_S - 1$. Here, $L = 1$ and then $N_S = M$. Then, assuming that the gain and offset are already canceled as in (22), the sampled signal with timing mismatch is

$$r_k(nT_c) = b_k p(nT_c - kT_r + \Delta t_n) + \eta_k(nT_c) \tag{28}$$

By averaging and multiplicating by the known b_ks, (24) becomes

$$\hat{r}(nT_c) = \frac{1}{K_P}\sum_{k=1}^{K_P} b_k^2 p(nT_c - kT_r + \Delta t_n) + \eta_k(nT_c) \tag{29}$$

So the averaged pulses can be approximated as in (25).

These results can be extended for a RMPF channel with impulse response $h(t)$ given by (4) as follows. As stated in Section II, the received signal in a time window covering the transmission pulse repetition rate T_r is defined by (5), assuming synchronization and channel estimation. In addition, the ideally-sampled received signal at the output of the RF front-end analog filter at sampling rate T_c is given by (8). Now, let us assume $N_S = ML$ such that we have M samples per pulse replica in the received kth frame. We now assume that gain and offset mismatch have already been estimated and compensated for, and that a good estimation of the channel impulse response is available. Considering the timing mismatch as in the AWGN channel case, the received bit is

$$r_k(nTc) = b_k \sum_{l=0}^{L-1} c_l(nT_c) p(nT_c + \Delta t_n - l/W - kT_r) + \eta_k(nT_c) \tag{30}$$

Then, we can multiply each replica in (30) by the complex conjugate of the channel coefficient $c_l(nT_c)$ in order to recover the phase of the pulse, and then divide by $\|c_l\|^2 = c_l c_l^*$ to normalize the amplitude. Then, including averaging over K_P bits of a training (pilot) signal and using a delay line with a time step $1/W$, we get the averaged pulse as

$$\hat{r}(nT_c) = \frac{1}{K_P}\sum_{k=1}^{K_P}\frac{b_k^2}{L}\sum_{l=0}^{L-1} p(nT_c + \Delta t_n - l/W - kT_r) + \eta_k(nT_c) \tag{31}$$

Again, this can be approximated as (25), where we now have $K_P L$ averaged pulses instead of only K_P because we can include the pulse replicas in the estimation.

As UWB channel models can be essentially described as a certain number of exponentially decaying clusters (say C) of multipath components with a certain number of exponentially decaying resolvable paths (say L), they can also be considered in this analysis and the main difference is the addition of another summation over C in equations (30)-(31) to add the contribution of the different clusters [23].

Note from (31) that as long as b_i is known, more pulses can be added to the average calculation to improve the estimator performance. Therefore, once the bits have been detected, they can be used in (31) to update the timing mismatch estimation which also allows to track changes in the different Δts.

B. TIMING MISMATCH ESTIMATION

In the equation describing the gaussian pulse (2), t_0 is a causalization constant such that the center peak of the gaussian bell occurs at $t = t_0$. If we consider that the pulse bandwidth W is 10 dB below the maximum of its Fourier transform [2], the we can compute T_0 as

$$T_0 = \sqrt{\frac{\ln(10)}{4\pi W^2}} \cong \frac{1}{2.35W} \tag{32}$$

For a unitary pulse amplitude, $K_0 = \sqrt{2}T_0$. With this calculations, we can write $p(t)$ as

$$p(t) = e^{-\frac{\pi}{2}\left(\frac{t-t_0}{T_0}\right)^2} \tag{33}$$

which is a gaussian bell with mean t_0 and standard deviation $\sigma = T_0$. Then, if we define a minimum sampling period slightly higher than the Nyquist rate $T_c = T_0 \cong 1/(2.35W)$ and consider N samples per pulse, then $t_0 = (N/2)T_c$. Let's consider we want to sample the gaussian pulse with a deviation up to 4σ from the center peak t_0. After N samples, $t_N = NT_c = t_0 + 4\sigma$. Replacing $\sigma = T_c$ and $t_0 = (N/2)T_c$, we can solve the equation for N, which gives $N = 8$.

Then, we can estimate $t = nT_c + \Delta t_n$ from (25) and (33) for the nth ADC averaged output samples as

$$\hat{t} = t_0 \pm \sqrt{-\frac{2T_0^2}{\pi}\ln(\hat{r})} \tag{34}$$

such that $\Delta\hat{t}_n = \hat{t} - nT_c$. In (34), we take the "$-$" for the square root if $n < N/2$ and the "$+$" otherwise. Note that as t_0 denotes the center of the pulse, the negative square root in (34) is used to obtain $\hat{t}$ for the first half of the pulse samples, while the positive part gives the estimates for the second half.

The complete estimation process is shown in Fig. 3, and can be summarized as follows:

- *Step 1:* After the received signal $r_k(nT_c)$ is acquired, the estimated bit b_k is calculated by (9) and (10).
- *Step 2:* The pulse samples are multiplied by b_k and averaged as in (24) to obtain (25).
- *Step 3:* Equations (25) and (33) are used to obtain $\hat{t}$ as in (34).

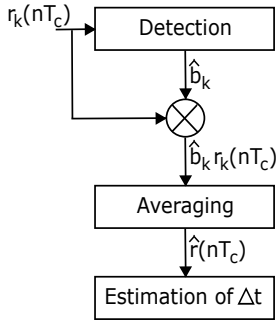

FIGURE 3. Diagram of the estimation process and the signals involved.

C. LOWER BOUND ON REQUIRED ADC RESOLUTION

The required time resolution of the template to obtain a good estimate is related both to the ADC bit resolution and the slope of the pulse

$$\Delta t = t_{i+1} - t_i = \frac{\Delta A_{min}}{s(t_i)} \tag{35}$$

where $s(t_i)$ is the slope of the pulse at time t_i and ΔA_{min} is the least significant bit (LSB) of the ADC which can be expressed as a function of the ADC resolution B as

$$\Delta A_{min} = LSB = \frac{A_{max}}{2^B - 1} \tag{36}$$

Then, considering a normalized template ($A_{max} = 1$),

$$\Delta t = \frac{1}{s(t_i)(2^B - 1)} \tag{37}$$

In order to get a good estimate of the timing mismatch error, the time resolution of the used template should be as high as possible. Suppose we wish a time resolution $\Delta t \leq MT_c/100$ such that the timing mismatch estimation falls within 1% of T. Then, the condition is

$$B \geq \log_2\left(\frac{100}{s(t_i)MT_c} + 1\right) \cong \log_2(100) - \log_2(s(t_i)MT_c) \tag{38}$$

If $s(t_i)MT_c \in [0, 1]$, $\log_2(s(t_i)MT_c) < 0$ and the required resolution is $B > \log_2(100) = 6.64$. Therefore, for a certain resolution B, the error will be smaller at those samples where the slope of the pulse is higher.

V. TI ADC COMPENSATION

Compensation of gain and offset mismatch errors in TI-ADCs can be easily accomplished [11] by first subtracting the estimated offset from the output samples of each ADC, and then multiplying by the inverse of the estimated gain error. As the timing shifts have previously been estimated with the method described in Section IV and the overall ideal sampling frequency is known, we have available the following data,

- The actual instants where samples are being taken in each ADC ($t_m[k] = kT + \Delta t_m$).
- The value of the samples taken at the actual time instants after correcting for offset and gain error $\hat{r}_{adm}[k]$.

- The ideal sampling instants with no timing mismatches $t[n] = nT/M$.

Therefore, we can estimate the samples that would have been taken at the ideal time instants through interpolation between the available samples using the available timing information. To that purpose, we propose the use of a simplified form of the Lagrange interpolation polynomial, as discussed in [11]. This leads to a time-varying filter implementation. The coefficients of the resulting time-variant filter are known, so the computational complexity is in the order of that of an FIR filter. Our goal is to test the estimation process proposed in Section IV and analyze the performance of the system with and without compensation. However, other compensation methods such as fractional delay filters [27] or spline interpolation [28] could also be used.

Lagrange interpolation is composed of a set of N orthonormal polynomials of Nth order. Then, given a function $f(t)$ and a data set $f(t_1), \cdots, f(t_N)$, the nth polynomial described by

$$P_n(t) = \prod_{\substack{j \neq n \\ j=1}}^{N} \left[\frac{t - t_j}{t_n - t_j} \right] \tag{39}$$

satisfies $P_n(t) = 1$ if $t = t_n$ and $P_n(t) = 0$ for $t = t_j, j \neq n$. Hence, the polynomial defined as

$$P(t) = \sum_{n=1}^{N} P_n(t) f(t_n) \tag{40}$$

is an approximation for $f(t)$ in the given interval, defined by the available data set.

It is clear from (39) and (40) that $P(t_n) = f(t_n), n = 1, \cdots, N$. The approximation of $f(t)$ by $P(t)$ will be better at the center of the interval of data samples used for fitting the polynomial (around $t_{N/2}$) and the approximation will be more accurate for higher N. However, if N is high, convergence problems will arise in the borders, i. e. around t_1 and t_N.

In TI-ADCs, $f(t_n)$ is the output sample of the TI-ADC array after correcting for gain and offset mismatches, and $t_n = nT + \Delta t_m$ is the sampling instant at the periodic but nonuniform time interval defined by the sampling frequency of each ADC and the (previously estimated) sampling shift Δt_m in the mth ADC. Hence, we use the Lagrange interpolation polynomial to estimate $f(t)$ at the correct sampling instant t.

VI. COMPARATIVE ANALYSIS

In this section, we compare the approach for timing mismatch error estimation proposed in this work and that of three representative alternatives found in the literature. These alternatives include: off-line estimation [11], blind estimation [18], and mixed-mode analog-digital solutions [6]. The comparative analysis include the accuracy of estimation results, computational complexity and convergence speed. As previously stated in the introduction, we show that our approach achieves high quality estimates when compared to blind and mixed-mode methods with lower computational complexity than off-line estimation.

Table I shows the main features of each method and the differences between them in a conceptual manner. Here, the computational complexity is roughly estimated based on the additional signal processing required for each technique to obtain the mismatch error estimates. Clearly, the blind and off-line approaches require intensive signal processing before the estimation algorithm can be performed when compared to our approach and the mixed mode proposal. Convergence speed and accuracy are roughly estimated based on the type of estimation algorithms used. The least squares algorithm used in the off-line method provides fast convergence and higher accuracy (with lower variance of the estimates [11]) compared with the gradient-based algorithms of blind methods (where the accuracy is mainly determined by the update step and the quality of the cost function to be minimized). The mixed mode technique involves a slow iteration process, where the analog delay paths (whose time resolution determines the precision of the estimates) have to be repeatedly adjusted through all possible combinations until a decrease in the mean squared error MSE is observed in the digital domain. In our proposal, we compare the averaged received pulses with a clean template and obtain a better estimate in each iteration.

Now that we gave an idea of what to expect regarding complexity and accuracy in a qualitative manner, we provide some quantitative computational complexity analysis based on the most intensive processing part of each approach.

In [11], the most intensive calculations are associated to the sine-wave fitting algorithm used to compute the reference signal. Here, we used blocks of $N_S = 8196$ output data samples from the ADC under test for several sinusoid input signals of different frequencies. We simulated (off-line) a set of ideal sinusoids for each analyzed input frequency and performed sequential searches varying phase, amplitude and frequency of the ideal sinusoid until a good fit to the sampled data was obtained by minimization of the MSE. For the phase search, a resolution of $2\pi/360$ between $[0, 2\pi]$ was used, leading to the generation of 360 sinusoids of 8196 points. Once the phase minimizing the error was obtained, it was fixed and used to estimate the other parameters. For amplitude and frequency adjustment, we used 100 values to perform the search around 10% of their expected values, which adds 200 more sinusoids to the search. The MSE was used as measure, and it is computed as

$$\epsilon^2 = \frac{1}{N_S} \sum_{n=1}^{N_S} [y(n) - \hat{y}_f(n)]^2 \tag{41}$$

where $y(n)$ represents the sampled data and $\hat{y}_f(n)$ the sinusoid used for fitting, respectively. The computation of (41) involves N_S subtractions, N_S multiplications and one division for each parameter variation, which leads to a total of $560N_S$ subtractions, $560N_S$ multiplications, and 560 divisions. However, once the reference signal is obtained,

TABLE 1. Main characteristics of representative approaches.

Method	Domain	Trainig signal	Additional processing	Accuracy	Complexity	Convergence
Off-line estimation [11]	Digital	Yes	Sine-wave fitting	High	High	Fast
Blind estimation [18]	Digital	No	FFT, Hilbert transform, frequency shifting	Moderate	High	Slow
Mixed mode [6]	Mixed	No	Link MMSE calculation	Moderate	Moderate	Slow
Pilot based (this work)	Digital	Pilot tones	Averaging	High	Moderate	Fast

estimation of the mismatch parameters is quite fast, accurate, and straightforward.

We now analyze the computational complexity associated to the estimation of the mismatch parameters of the blind method in [18]. Here, we compute the complexity in terms of operations per iteration, multiplied by the number of iterations needed to achieve convergence. We consider only the LMS algorithm (for simplicity), which involves the calculation of 4 coefficients per channel ADC, resulting in 3 multiplications and one addition per coefficient for each iteration. Then, for an M channel TI-ADC this results in $12M$ multiplications and $4M$ additions per iteration. According to [18] and our own simulations, convergence is reached after $N_I = 40000$ iterations, leading to $12MN_I$ multiplications and $4MN_I$ additions. This computational complexity is similar to that of [11] if we consider $M = 8$.

The complexity of the method in [6] can be computed as follows. We consider an M channel TI-ADC with N_D possible adjustable analog delays for each channel ADC and N_S samples used for MSE calculation in the digital domain for each possible combination of analog delays. Then, the number of possible combinations are $N_C = (N_D M)!/(N_D M - M)!M!$. Considering an MSE calculation as in (41) for each possible combination, we get $N_C N_S$ multiplications, $N_C N_S$ subtractions, and N_C divisions.

In the approach presented in this work, the number of operations can be calculated from (22), (24) and (34). This lead to $K_P LM$ additions, K_P multiplications and 2 divisions for (24), plus $3M$ multiplications, M divisions, additions, and square roots for (34). The results are summarized in Table II.

TABLE 2. Computational complexity of representative approaches.

Method	Multiplications	Additions	Divisions
Off-line estimation [11]	$560N_S$	$560N_S$	560
Blind estimation [18]	$12MN_I$	$4MN_I$	-
Mixed mode [6]	$N_C N_S$	$N_C N_S$	N_C
Pilot based (this work)	$K_P + 3M$	$K_P LM + M$	$M + 2$

VII. SIMULATION RESULTS

We assess the effect of ADC resolution on the performance of the receiver, as well as ADC induced distortion for the case of mismatch errors in a TI-ADCs. In addition, we analyze detection performance in terms of BER as a function of SNR and ADC resolution, and evaluate the performance loss due to ADC induced distortion. We also show the behavior of the system after compensation. In this case, we consider an 8-branch TI-ADC with 8 bits of resolution and 15% gain, offset and timing mismatches. The mismatches were simulated as random values with a maximum deviation of 15% from unitary gain, normalized amplitude, and individual ADC sampling period, respectively. We also analyze the signal to noise and distortion ratio (SINAD) at the output of the ADC (which is proportional to the effective number of bits - ENOB) as a function of SNR before and after compensation. We consider an AWGN channel as a reference for the best case scenario, while a RMPF channel is simulated as a more realistic and general transmission media. In the case of a RMPF channel, we assume $L = 5$ resolvable paths with equal power rays, and that the channel impulse response described by equation (4) is time invariant over several transmitted pulses. Then, it can change in a random fashion.

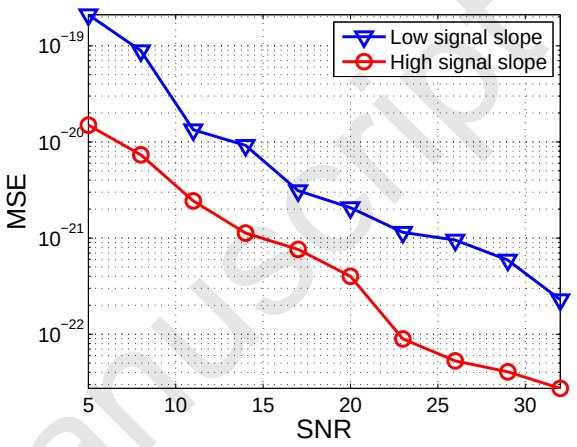

FIGURE 4. MSE for two estimated timing mismatches.

A. ON-LINE TIMING MISMATCH ESTIMATION RESULTS

Figure 4 shows the $MSE = (1/N)(\Delta t - \hat{\Delta t})^2$ of two estimated Δt with the method proposed in Section IV as a function of SNR (which for estimation purposes in this case is equivalent to adding more averaging in equation (31)). The estimated timing mismatch is calculated at a point of the gaussian pulse with low and high slope, respectively, for a training sequence of $2^{10} = 1024$ bits. The signal used for estimation is the received signal passed through the

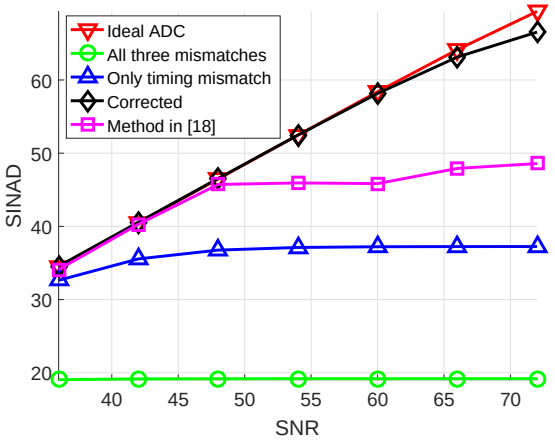

FIGURE 5. SNR at the input of the ADC and SINAD at its output for 15% mismatch errors.

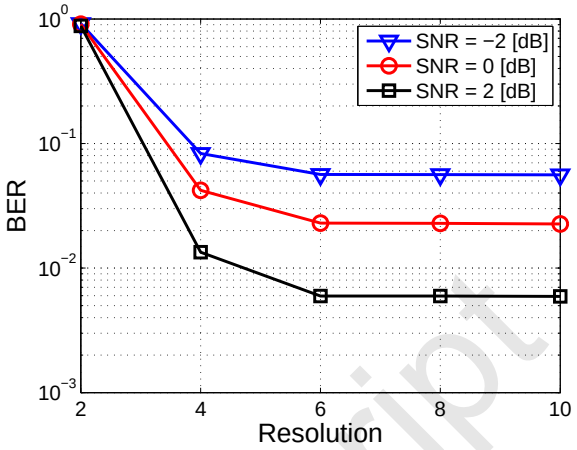

FIGURE 6. BER as a function of ADC resolution for 3 SNR scenarios for an OSR=2.

RMPF channel. As shown in the figure, the estimation error decreases as the SNR increases, independently of the slope of the pulse at the current sampling time. An SNR increment is also equivalent to an increment in the number of symbols used, either by using more pilots or adding the decoded bits for tracking as suggested in Section IV. This enhances the quality of the estimation as the averaging has the effect of lowering the variance of the noise term in (24).

B. ADC PERFORMANCE

Figure 5 shows the SNR at the input of the ADC and the obtained SINAD at its output before and after compensation with the proposed method, compared to the performance of an ideal ADC. Note that without distortion in the ADC, both should be equal, as the SNR at the output of the ADC in that case is determined by the SNR at its input. We also show the performance of the ADC after gain and offset compensation but before cancellation of timing mismatch errors. We can see from the figure that the three mismatch errors combined severely deteriorate the performance of the converter in terms of SINAD and therefore effective resolution (ENOB), which can be computed as $ENOB \cong (SINAD - 1.76)/6.02$. Then, the effective resolution is 3 bits without correction for all the simulated SNR scenarios and 6 bits when only timing mismatch errors are considered. Therefore timing mismatch compensation is also required to restore close to ideal performance. The proposed method was simulated with data affected by AWGN and RMPF channels. As the results coincide, we show only those obtained for the RMPF channel simulation.

We also show the results obtained by applying the correction method in [18], where we can see that correction performance is lower than that of our proposal when the input SNR is beyond 48 dB. This is explained by the fact that convergence of the method in [18] is sensitive to the update step μ in the LMS algorithm. While a larger step will lead to faster convergence with higher error, the algorithm convergence is much slower and even fails if the step is too small. As in all gradient-based algorithms, the error after convergence is in the order of the update step, which in this case allows a maximum SNR of 48 dB. The work from [18], also resulted to be very sensitive to AWGN at its input. Even in the presence of low levels of noise, the algorithm fails to converge. For this reason, we analyzed its performance with noiseless inputs only affected by mismatch errors and quantization noise for different resolutions to include the results.

The method in [11] has the same compensation performance, but at the cost of foreground off-line estimation of the mismatch parameters, i.e. the only difference is the additional computational cost in the estimation process and the fact that the ADC operation must be stopped in order to do so. Therefore, we didn't include the results in the figure. The method in [6] is tied both to the calibration hardware and the ADC implemented on the same chip, which has a fixed nominal resolution of 6 bits. This resolution is equivalent to the ADC performance before compensation of timing errors in the simulated scenario, which makes the comparison unfair in this context.

C. RESOLUTION

Figures 6 and 7 show the BER as a function of ADC resolution for 3 different SNR levels and two OSR values which are 2 and 5 when transmitting over an AWGN channel. In this case it can be seen that the BER drops as a function of ADC resolution until 6 bits are reached, and remains constant for higher resolutions. It can also be seen that when oversampling can be allowed, it offers a significant boost in detection performance. Another interesting fact is that quantization with two bits translates in a poor performance independently of SNR and OSR, while quantization with 4-6 bits results in good BER behaviour. The goal of this simulation in particular is to show that ADC resolution plays an important role in BER performance even for low SNR

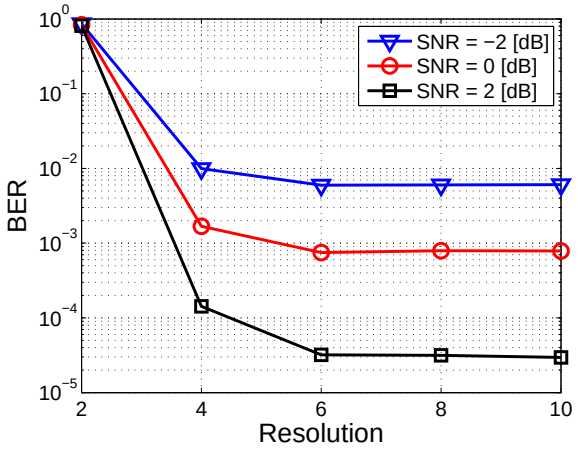

FIGURE 7. BER as a function of ADC resolution for 3 SNR scenarios for an OSR=5.

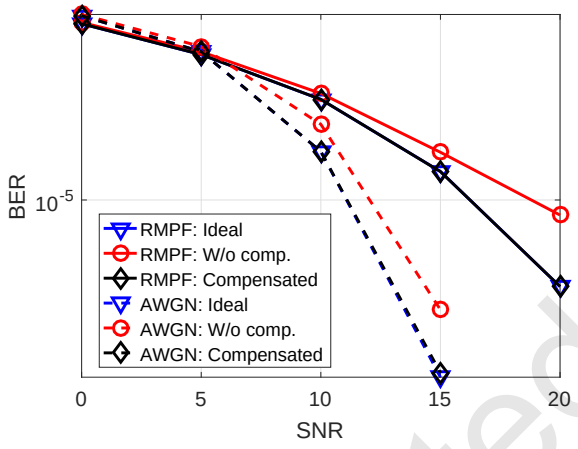

FIGURE 8. BER as a function of SNR and 15% mismatch errors for RMPF (solid line) and AWGN (dashed line) channels.

scenarios, and oversampling leads to enhanced detection. The results for a wider range of SNRs without oversampling are shown in figures 5 and 8.

D. BER PERFORMANCE

Finally, Figure 8 shows the BER as a function of SNR for the case of both AWGN and RMPF channels. Simulations include BER for an ideal ADC, and for the TI-ADC with 15% mismatch errors before and after compensation using the proposed estimation technique. As expected, good performance is restored after correction, which shows the effectiveness of the proposed method and the importance of ADC correction for error reduction at the receiver.

VIII. CONCLUSIONS

We have introduced a novel timing mismatch estimation technique in the context of an IR-UWB receiver. The estimation technique is pilot-based, allowing for on-line background estimation with tracking capabilities. We also derived a lower bound on the required ADC resolution to attain a certain estimation precision, showing the feasibility of the proposed method. As demonstrated by simulation results, timing mismatch estimation and correction is critical to achieve good performance both in terms of ADC effective resolution and BER performance of the receiver, even when considering that gain and offset errors have been previously corrected.

REFERENCES

[1] A. Yassin, Y. Nasser, M. Awad, A. Al-Dubai, R. Liu, C. Yuen, and R. Raulefs, "Recent advances in indoor localization: A survey on theoretical approaches and applications," IEEE Communications Surveys Tutorials, vol. PP, no. 99, pp. 1–1, 2016.

[2] A. M. Tonello, F. Versolatto, and M. Girotto, "Multitechnology (I-UWB and OFDM) coexistent communications on the power delivery network," IEEE Transactions on Power Delivery, vol. 28, pp. 2039–2047, Oct 2013.

[3] H. ZEMMOUR, G. Baudoin, and A. Diet, "Soil effects on the underground to aboveground communication link in ultra wideband wireless underground sensor networks," IEEE Antennas and Wireless Propagation Letters, vol. PP, no. 99, pp. 1–1, 2016.

[4] A. Buchwald, "High-speed time interleaved ADCs," IEEE Communications Magazine, vol. 54, pp. 71–77, April 2016.

[5] S. M. R. Islam, N. Avazov, O. A. Dobre, and K. S. Kwak, "Power-domain non-orthogonal multiple access (NOMA) in 5G systems: Potentials and challenges," IEEE Communications Surveys Tutorials, vol. PP, no. 99, pp. 1–1, 2016.

[6] B. T. Reyes, R. M. Sanchez, A. L. Pola, and M. R. Hueda, "Design and experimental evaluation of a time-interleaved ADC calibration algorithm for application in high-speed communication systems," IEEE Transactions on Circuits and Systems I: Regular Papers, vol. 64, pp. 1019–1030, May 2017.

[7] C. R. Anderson, S. Venkatesh, J. E. Ibrahim, R. M. Buehrer, and J. H. Reed, "Analysis and implementation of a time-interleaved ADC array for a software-defined UWB receiver," IEEE Transactions on Vehicular Technology, vol. 58, pp. 4046–4063, Oct 2009.

[8] R. V. de Plassche, CMOS Integrated Analog-to-Digital and Digital-to-Analog Converters. Dordrecht, The Netherlands: Kluwer Academic, 2003.

[9] S. Ponnuru, M. Seo, U. Madhow, and M. Rodwell, "Joint mismatch and channel compensation for high-speed OFDM receivers with time-interleaved ADCs," IEEE Trans. Comm., vol. 58, pp. 2391–2401, Aug. 2010.

[10] V. T. D. Huynh, N. Noels, and H. Steendam, "Offset mismatch calibration for TI-ADCs in high-speed OFDM systems," in 2015 IEEE Symposium on Communications and Vehicular Technology in the Benelux (SCVT), pp. 1–5, Nov 2015.

[11] C. A. Schmidt, J. E. Cousseau, J. L. Figueroa, B. T. Reyes, and M. R. Hueda, "Efficient estimation and correction of mismatch errors in time-interleaved ADCs," IEEE Transactions on Instrumentation and Measurement, vol. 65, pp. 243–254, Feb 2016.

[12] S. K. Sindhi and K. M. M. Prabhu, "Reconstruction of N-th order nonuniformly sampled bandlimited signals using digital filter banks," Digital Signal Processing, vol. 23, pp. 1877–1886, June 2013.

[13] J. Elbornsson, F. Gustafsson, and J. E. Eklund, "Blind adaptive equalization of mismatch errors in a time-interleaved A/D converter system," IEEE Transactions on Circuits and Systems I: Regular Papers, vol. 51, pp. 151–158, Jan 2004.

[14] C. Vogel and H. Johansson, "Time-interleaved analog-to-digital converters: status and future directions," in Circuits and Systems, 2006. ISCAS 2006. Proceedings. 2006 IEEE International Symposium on, pp. 4 pp.–3389, 2006.

[15] C. Vogel, M. Hotz, S. Saleem, K. Hausmair, and M. Soudan, "A review on low-complexity structures and algorithms for the correction of mismatch errors in time-interleaved ADCs," in New Circuits and Systems Conference (NEWCAS), 2012 IEEE 10th International, pp. 349–352, 2012.

[16] P. Benabes, C. Lelandais-Perrault, and N. L. Dortz, "Mismatch calibration methods for high-speed time-interleaved ADCs," in 2014 IEEE 12th International New Circuits and Systems Conference (NEWCAS), pp. 49–52, June 2014.

[17] J. Elbornsson, F. Gustafsson, and J. Eklund, "Blind equalization of time errors in a time-interleaved ADC system," IEEE Trans. Signal Process., vol. 53, pp. 1413–1424, Apr. 2005.

[18] Y. Qiu, Y. J. Liu, J. Zhou, G. Zhang, D. Chen, and N. Du, "All-digital blind background calibration technique for any channel time-interleaved ADC," IEEE Transactions on Circuits and Systems I: Regular Papers, vol. PP, no. 99, pp. 1–12, 2018.
[19] S. Chen, L. Wang, H. Zhang, R. Murugesu, D. Dunwell, and A. C. Carusone, "All-digital calibration of timing mismatch error in time-interleaved analog-to-digital converters," IEEE Transactions on Very Large Scale Integration (VLSI) Systems, vol. 25, pp. 2552–2560, Sept 2017.
[20] Y. Liu, Z. Tan, H. Hu, L. J. Cimini, and G. Y. Li, "Channel estimation for ofdm," IEEE Communications Surveys Tutorials, vol. 16, pp. 1891–1908, Fourthquarter 2014.
[21] S. Kwon, S. Lee, and J. Kim, "A joint timing synchronization, channel estimation, and SFD detection for IR-UWB systems," Journal of Communications and Networks, vol. 14, pp. 501–509, Oct 2012.
[22] F. A. Dietrich and W. Utschick, "Pilot-assisted channel estimation based on second-order statistics," IEEE Transactions on Signal Processing, vol. 53, pp. 1178–1193, March 2005.
[23] M. G. D. Benedetto and G. Giancola, Understanding ultra wide and radio fundamentals. Upper Saddle River, New Jersey, U.S.: Prentice Hall PTR, 2004.
[24] J. G. Proakis, Digital Communications - Fourth Edition. McGraw Hill, 2001.
[25] A. M. Tonello and R. Rinaldo, "A time-frequency domain approach to synchronization, channel estimation, and detection for DS-CDMA impulse-radio systems," IEEE Transactions on Wireless Communications, vol. 4, pp. 3018–3030, Nov 2005.
[26] P. P. Vaidyanathan, Multirate Systems and Filter Banks. Engelwood Cliffs, New Jersey 07632, US: Prentice Hall PTR, 1993.
[27] T. Laakso, V. Valimaki, M. Karjalainen, and U. Laine, "Splitting the unit delay [FIR/all pass filters design]," Signal Processing Magazine, IEEE, vol. 13, pp. 30–60, Jan 1996.
[28] G. Qin, G. Liu, M. Gao, X. Fu, and P. Xu, "Correction of sample-time error for time-interleaved sampling system using cubic spline interpolation," Metrology and Measurement Systems, vol. 21, pp. 485–496, Aug. 2014.

CHRISTIAN A. SCHMIDT received the B.Sc. degree in Electronic Engineering and the Ph.D. degree in Engineering from Universidad Nacional del Sur, Bahía Blanca, Argentina, in 2005 and 2012, respectively. Since 2015, he holds a position as researcher at Consejo Nacional de Investigaciones Científicas y Técnicas (CONICET). From december 2018 he is also with the IETR-INSA Rennes, France. His research interests include nonlinear dynamic systems modeling and compensation, post-processing techniques for distortion reduction in Analog-to-digital converters, and signal processing for communications systems including OFDM, UWB, Full-duplex and massive MIMO.

JOSÉ L. FIGUEROA (M'98–SM'01) received the B.Sc. degree in electrical engineering and the Ph.D. degree in systems control from the Universidad Nacional del Sur, Bahía Blanca, Argentina, in 1987 and 1991, respectively. He has been with the Universidad Nacional del Sur and the National Scientific and Technical Research Council of Argentina since 1995. His current research interests include control systems and signal processing.

JUAN E. COUSSEAU received the B.Sc from the Universidad Nacional del Sur (UNS), Bahia Blanca, Argentina, in 1983, the M.Sc. degree from COPPE/ Universidade Federal do Rio de Janeiro (UFRJ), Brazil, in 1989, and the Ph.D. from COPPE/UFRJ, in 1993, all in electrical engineering. Since 1984, he has been with the undergraduate Department of Electrical and Computer Engineering at UNS, and with the graduate Program since 1994. He is a senior researcher of the National Scientific and Technical Research Council (CONICET) of Argentina. He has been involved in scientific and industry projects with research groups from Argentina, Brazil, Spain, USA, Finland and South Africa. He is coordinator of the Signal Processing and Communication Laboratory (LaPSyC) at UNS (http://lapsyc.ingelec.uns.edu.ar). He is Senior member of the IEEE. He was IEEE Circuits and Systems Chair of the Argentine Chapter, from 1997 to 2000, and member of the Executive Committee of the IEEE Circuits and Systems Society during 2000/2001 (Vice-president for Region 9). He participates of the IEEE Signal Processing Society Distinguished Lecturer Program 2006. He is currently Director of the Instituto de Investigaciones en Ingeniería Eléctrica - Alfredo Desages, CONICET-UNS (http://www.iiie.uns.edu.ar). His research interests are related to adaptive and statistical signal processing with application to modern broadband wireless communications.

ANDREA M. TONELLO received the laurea degree in electrical engineering (summa cum laude) and the doctorate of research degree in electronics and telecommunications from the University of Padova, Padova, Italy, in 1996 and in 2002, respectively. From 1997 to 2002, he was with Bell Labs-Lucent Technologies, Whippany, NJ, USA, first as a Member of the Technical Staff. Then, he was promoted to Technical Manager and appointed to Managing Director of the Bell Labs Italy division. In 2003, he joined the University of Udine, Udine, Italy, where he became Aggregate Professor in 2005 and Associate Professor in 2014. Currently, he is Professor at the Chair of Embedded Communication Systems of the University of Klagenfurt, Klagenfurt, Austria. Dr. Tonello received several awards, including the Bell Labs Recognition of Excellence Award (1999), the Distinguished Visiting Fellowship from the Royal Academy of Engineering, U.K., in 2010, the IEEE Distinguished Lecturer Award from VTS in 2011-2015 and from COMSOC in 2018-2019, the Italian Full Professor Habilitation (2013), the Chair of Excellence from Carlos III Universidad, Madrid (2019-20). He is also the co-recipient of nine best paper awards. He was the Chair of the IEEE Communications Society Technical Committee on Power Line Communications and was/is Associate Editor of several journals including IEEE Trans. on Vehicular Tech., IEEE Trans. on Comm., and IEEE Access.